

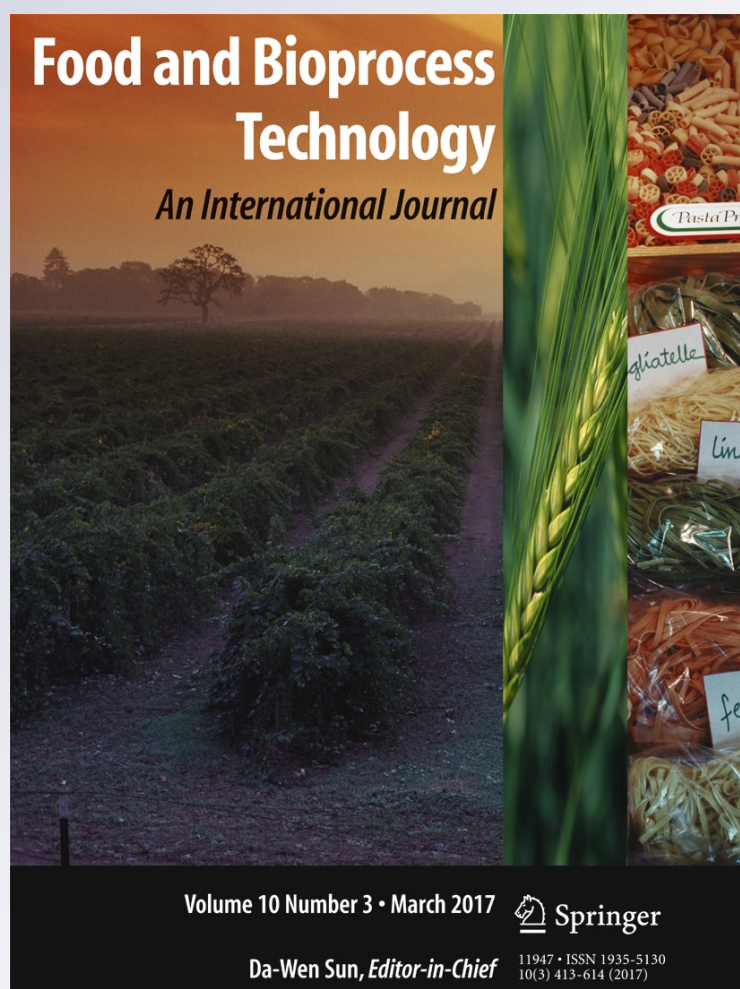
# *Encapsulation and Stabilization of $\beta$ -Carotene in Amaranth Matrices Obtained by Dry and Wet Assisted Ball Milling*

**Diego F. Roa, M. Pilar Buera, Marcela P. Tolaba & Patricio R. Santagapita**

**Food and Bioprocess Technology**  
An International Journal

ISSN 1935-5130  
Volume 10  
Number 3

Food Bioprocess Technol (2017)  
10:512-521  
DOI 10.1007/s11947-016-1830-y



**Your article is protected by copyright and all rights are held exclusively by Springer Science +Business Media New York. This e-offprint is for personal use only and shall not be self-archived in electronic repositories. If you wish to self-archive your article, please use the accepted manuscript version for posting on your own website. You may further deposit the accepted manuscript version in any repository, provided it is only made publicly available 12 months after official publication or later and provided acknowledgement is given to the original source of publication and a link is inserted to the published article on Springer's website. The link must be accompanied by the following text: "The final publication is available at [link.springer.com](http://link.springer.com)".**



# Encapsulation and Stabilization of $\beta$ -Carotene in Amaranth Matrices Obtained by Dry and Wet Assisted Ball Milling

Diego F. Roa<sup>1</sup> · M. Pilar Buera<sup>1,2,3</sup> · Marcela P. Tolaba<sup>1</sup> · Patricio R. Santagapita<sup>1,2,3</sup>

Received: 13 May 2016 / Accepted: 17 November 2016 / Published online: 2 December 2016  
© Springer Science+Business Media New York 2016

**Abstract** Amaranth starchy fractions have recently awakened interest from the industry, mainly due to its potential functional characteristics. The encapsulating efficiencies of starch-enriched fraction (SEF) and native starch (NS) obtained, respectively, by dry and wet assisted ball milling were studied. The effects of high impact milling, gelatin addition, and storage temperature (5–45 °C, 45 days) on the retention of  $\beta$ -carotene were investigated. Significant effects of both milling and amaranth protein present in SEF matrix on emulsification and subsequent retention of  $\beta$ -carotene were found. Ball milled SEF matrix showed the best encapsulation performance, with up to three times of total  $\beta$ -carotene content in comparison with the NS-containing matrices. Degradation of surface and encapsulated  $\beta$ -carotene followed a first-order kinetic model and was strongly influenced by storage temperature. The activation energy of surface  $\beta$ -carotene degradation doubled that of encapsulated  $\beta$ -carotene (86 vs. 48 kJ/mol,

respectively). This difference indicates that encapsulated  $\beta$ -carotene is more stable to temperature changes than surface  $\beta$ -carotene and revealed the protective capability of the SEF matrix even at high temperatures. The color coordinates  $a^*$  and  $L^*$  for samples stored at 25 and 45 °C positively correlated with the remaining  $\beta$ -carotene, revealing the potentiality of color measurement as an adequate index of  $\beta$ -carotene retention. The starch-enriched amaranth fraction modified by high impact milling showed a high technological potential as an encapsulating agent and its own protein content served as a good emulsifier-stabilizer.

**Keywords** Encapsulating agent ·  $\beta$ -Carotene · Amaranth starch · Amaranth flour · Planetary ball milling · Thermal degradation

## Introduction

Recently, investigations on the different components of the amaranth grain, a pseudocereal produced in Andean region in South America, have been increased because of their functional properties for industrial and commercial use. Starch (48–62%) is the principal component of the amaranth grain. Starch granules composed mainly of amylose and amylopectin are spherical or polygonal (Saunders and Becker, 1984), with a very small diameter 0.5–2  $\mu\text{m}$  (Marcone, 2001), compared to other cereals (Breene, 1991). Amaranth starches present gelatinization temperatures within 65–83 °C depending on the grain variety and produce weak gels (Radosavljevic et al., 1998) due to their low amylose content (2.5%, Tari et al., 2003). Besides the known applications in the food industry (thickener for soups, fat replacer, pasta and baked products, among others; Kong et al., 2008), it has several uses in the

**Electronic supplementary material** The online version of this article (doi:10.1007/s11947-016-1830-y) contains supplementary material, which is available to authorized users.

✉ Patricio R. Santagapita  
prs@di.fcen.uba.ar

- <sup>1</sup> Departamento de Industrias, Facultad de Ciencias Exactas y Naturales, Universidad de Buenos Aires (FCEN-UBA), Intendente Güiraldes 2160, Buenos Aires C1428EGA, Argentina
- <sup>2</sup> Departamento de Química Orgánica, Facultad de Ciencias Exactas y Naturales, Universidad de Buenos Aires (FCEN-UBA), Buenos Aires, Argentina
- <sup>3</sup> Consejo Nacional de Investigaciones Científicas y Técnicas (CONICET), Buenos Aires, Argentina

manufacture of cosmetics, biodegradable films, and paper (Choi et al., 2004). Encapsulation of food ingredients or bioactive compounds can be relevant to many of these applications (Karathanos et al., 2007; Murua-Pagola et al., 2009). The choice of a matrix and its functional properties for encapsulation of antioxidants is very important to achieve high encapsulation efficiency and stability. Starches, maltodextrins, corn syrup, and gums have been used in technological processes in order to protect compounds of interest during processing and storage for their inclusion in foods. Because of its high availability and low cost, starches become a good choice for encapsulation (Madene et al., 2006). However, the native starch lacks of adequate functional properties for an effective encapsulation. Chemical or physical modifications of flours and starches have been applied in order to expand their technological use (Puncha-aron & Uttapap, 2013; Roa et al., 2014; Silva et al., 2012). Some researchers have chemically modified starches, obtaining high degrees of hydrolysis, which has resulted in an enhanced encapsulation capacity of these modified starches (Chattopadhyaya et al., 1998; Karathanos et al., 2007; Krishnan et al., 2005; Murua-Pagola et al., 2009; Wagner & Warthesen, 1995). Due to the low cost and environmental impact, physical processes are being used as pretreatment for the obtention and modification of flour and starches (Devi et al., 2009; Zhang et al., 2010). Ball milling is a unit operation that causes a sharp reduction in the average volume of the particles. In previous works, Roa et al. (2013, 2014) used a planetary ball mill in order to obtain modified amaranth flour and starches with different physicochemical properties in relation to native fractions. Through this treatment, changes in the degree of crystallinity, viscosity, thermal parameters, water absorption capacity, and solubility were obtained. Similar results were reported for rice, corn, and tubers (Chen et al., 2003; Devi et al., 2009; Huang et al., 2007; Jane et al., 1992; Morrison & Tester, 1994; Sanguanpong et al., 2003; Tamaki et al., 1998). Then, considering the low percentage of amylose of amaranth starch (2.5%, Tari et al., 2003) and the great impact on several properties caused by the intense grinding of the starch produced by ball milling, the use of high impact milling is proposed to provoke the breaking of amylopectin chains toward chains of low molecular weight (Morrison & Tester, 1994) in order to increase the encapsulating capacity of amaranth starch.

The aim of this study was to evaluate the ability of starchy amaranth fractions to encapsulate  $\beta$ -carotene (selected as model antioxidant). The effects of gelatin addition and high impact dry milling on emulsifying and encapsulating capabilities of amaranth matrices were determined. Temperature dependence of  $\beta$ -carotene thermal degradation (surface and encapsulated) was also investigated.

## Materials and Methods

### Materials

The amaranth grains (*Amaranthus cruentus*) provided by Cereales Naturales S.R.L (Lomas del Mirador, Argentina) were harvested in 2011 during spring from the west of Buenos Aires Province. The grains were manually selected in order to remove foreign matter and stored in sealed containers at 20 °C prior to their use. The moisture content of the grains was  $10.5 \pm 0.1$  g/100 g (AOAC 2000).

### Abrasive Milling

Starch-enriched fraction (SEF) was obtained by abrasive milling of the amaranth grains using a laboratory rice mill Suzuki MT-95 (Suzuki, Sao Pablo, Brazil), which separates automatically pearled amaranth (starchy fraction yield, 70%) and bran (lipid-protein fraction yield, 28%). Milling conditions involved 100 g of milling load and 90 min of milling time (Roa et al., 2013).

### Fraction Milling

The selection of milling energy levels was based on previous works in which the effect of milling energy on functional, and structural characteristics of amaranth fractions were analyzed (Roa et al., 2015, Roa et al., 2014). The selected energy levels correspond to mildly (2.5 kJ/g) and severely (6.5 kJ/g) milled amaranth fractions, achieved by wet and dry milling, respectively.

### Wet Milling

The SEF sample previously obtained by abrasive milling was milled in a planetary ball mill model PM-100 (Retsch, Haan Mettman, Germany) with one stainless steel milling cylinder (500 mL). The SEF sample and five times weight stainless steel balls (10 mm diameter) were placed into the stainless steel container up to about one third of their capacity. Soaking was performed into the stainless steel container with soaking solution of 0.3 g/L of NaOH (with NaOH from Sigma Chemical Co., St. Louis, MO, USA) and 0.2 g/L of sodium dodecyl sulfate (from J. T. Baker Co., NJ, USA) employing a solution:grain ratio of 1.2:1 (mL:g). The mill was rotated horizontally at constant milling speed of 400 rpm at 2.5 kJ/g of sample obtaining the homogenate. The ball milling was changed in rotational direction every 30 s. The homogenate was sifted through sieve no. 80 (177  $\mu$ m), no. 200 (74  $\mu$ m), and no. 0 (0  $\mu$ m) (Zonytest, model EJ200; Buenos Aires, Argentina). The residue (0  $\mu$ m) contained the starch slurry. Then, it was neutralized with HCl (1 N) and centrifuged in order to obtain starch. The isolated starch (NS) was freeze-



dried during 48 h at  $-56\text{ }^{\circ}\text{C}$  and 0.04 mbar in an ALPHA 1–4 LD2 freeze dryer (Martin Christ Gefriertrocknungsanlagen GMBH, Germany) and then stored at  $4\text{ }^{\circ}\text{C}$  temperature in a sealed container.

### Dry Milling

The SEF and NS samples previously obtained were pulverized in a planetary ball mill model PM-100 (Retsch) with one stainless steel milling cylinder (500 mL). The samples and five times weight stainless steel balls (10 mm diameter) were placed into the stainless steel container up to about one third of their capacity. The mill was rotated horizontally at constant milling speed of 400 rpm at 6.52 kJ/g of sample obtaining the milled native starch (NS/BM) and the milled starch-enriched fraction (SEF/BM). The ball milling was changed in rotational direction every 30 s.

### Matrices Preparation

A scheme of the matrices preparation is depicted in Fig. 1. The samples were suspended in distilled water (5% w/w) and heated in a thermostatic bath (Vicking SRL, Buenos Aires, Argentina) at  $95\text{ }^{\circ}\text{C}$  to obtain gelatinized starch paste. Trans- $\beta$ -carotene in oil was added to the cooled gelatinized starch paste in a ratio of 1:50 g:g on dry basis. The ratio between the core and wall material was chosen based on literature reports (Loksuwan, 2007; Matioli & Rodríguez-Amaya, 2002). The mixture was stirred until complete homogenization by using an Ultra-Turrax T18B (IKA®-WerkeGMBH & CO.KG, Staufen, Germany) at 15.500 rpm for 10 min. Then, the samples were quickly frozen using liquid nitrogen ( $-196\text{ }^{\circ}\text{C}$ ) and freeze-dried during 48 h at  $-56\text{ }^{\circ}\text{C}$  and 0.04 mbar in an ALPHA 1–4 LD2 freeze dryer (MartinChristGefriertrocknungsanlagen GMBH, Germany). Gelatin (0.05% w/w) (Ge, from Merck KGaA, Darmstadt, Germany) was added in some systems for comparative purposes (Fig. 1).

### Determination of the $\beta$ -Carotene Content

The procedure for determining surface and encapsulated  $\beta$ -carotene content is based on the fact that  $\beta$ -carotene is lipophilic and soluble in hexane, unlike the rest of the matrix components.

Surface  $\beta$ -carotene was extracted from the freeze-dried samples by washing them with 3 mL of hexane in a glass vial (5 mL) and shook in a Vortex-Genie 2 (Scientific Industry, Inc., Bohemia, NY, USA), at 1850 rpm for 8 min. The supernatant was measured at 452 nm using a spectrophotometer model V-630 UV-Vis (JASCO Inc., MD, USA). This wavelength was found to correspond to maximum absorbance of the spectrum from 200 to 600 nm and is in agreement with

previous results reported by Spada et al. (2012) and Sutter et al. (2007). The remaining matrix (without surface  $\beta$ -carotene) was dissolved by adding 1.5 mL of water and shook in a Vortex-Genie 2 at 1850 rpm for 2 min in order to release encapsulated  $\beta$ -carotene. Then, the encapsulated  $\beta$ -carotene was extracted with 3 mL of hexane and shook in a Vortex-Genie 2 at 1850 rpm for 6 min; the hexane fraction was measured at 452 nm. The concentration of  $\beta$ -carotene was calculated according to Eq. (1) and expressed as  $\text{mg/g}_{\text{matrix}}$ . An average value of three replicates was reported along with the standard deviation.

$$\text{Total } \beta\text{-carotene} \left( \frac{\text{mg}}{\text{g}_{\text{matrix}}} \right) = \frac{A \times MW \times DF \times 10^3 \times VH}{\varepsilon \times l \times SM} \quad (1)$$

where A is the absorbance at 452 nm, MW is the molecular weight of  $\beta$ -carotene (536.8 g/mol), DF is the dilution factor, VH is the volume of hexane (0.003 L),  $\varepsilon$  is the molar extinction coefficient of  $\beta$ -carotene in hexane (145,300 L/mol cm; Kimura & Rodríguez-Amaya, 2001), l is the path length (1 cm), and SM is the weight of starchy matrix in dry basis (0.04902 g).

### Encapsulation Performance

The emulsifying effect of proteins ( $5.0 \pm 0.1\%$ ) of the starch-enriched fraction (SEF) fraction was compared to that of the frequently employed gelatin (Ge). SEF and native starch (NS) milled fractions were used with and without gelatin (SEF/BM, SEF + Ge/BM; NS/BM; NS + Ge/BM). In addition, two non-milled matrices based on native starch were adopted as references (NS; NS + Ge).

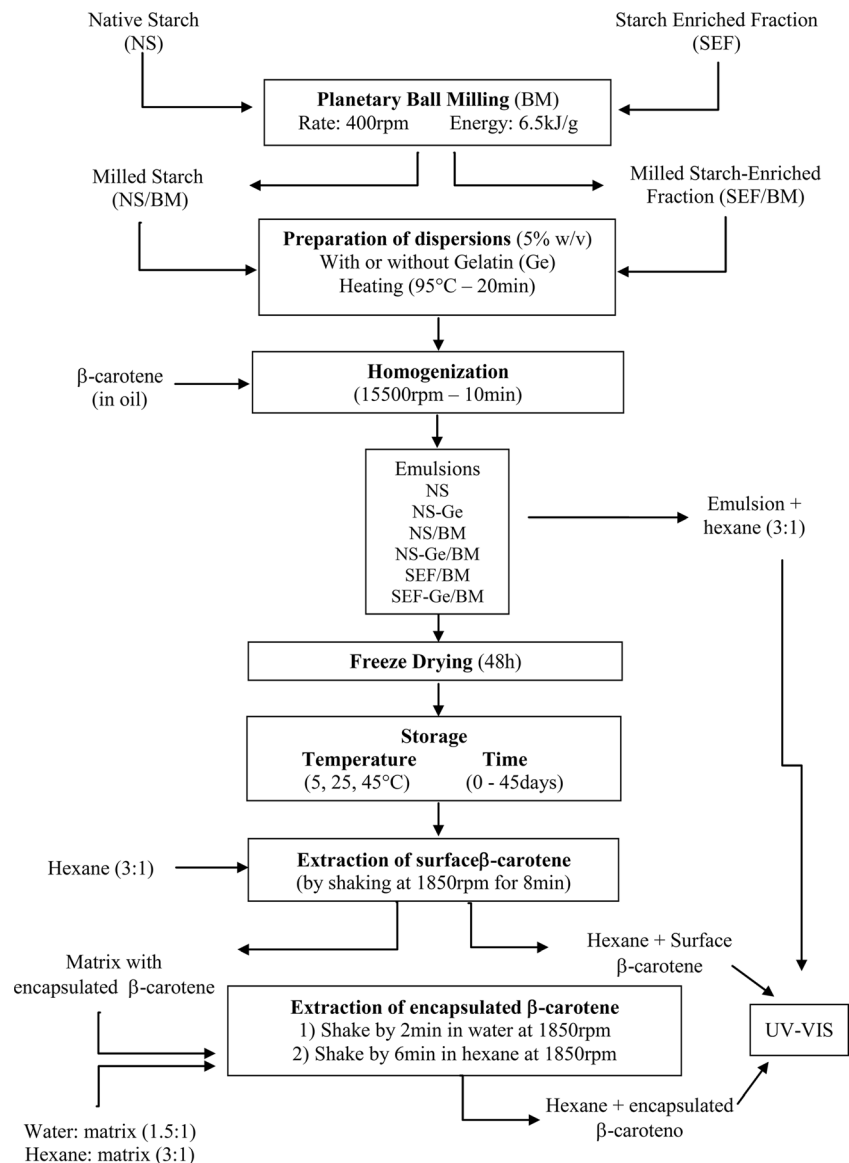
The encapsulation performance was calculated as the mass ratio between encapsulated and surface  $\beta$ -carotene.

### Thermal Treatments of Encapsulated Systems

The degradation of surface and encapsulated  $\beta$ -carotene in the presence of headspace oxygen was studied. The samples were stored at  $5\text{ }^{\circ}\text{C}$  in a conventional fridge and at 25 and  $45\text{ }^{\circ}\text{C}$  in a forced air oven SR71 model (FAC SRL, Buenos Aires, Argentina), using similar storage conditions as reported by Tang & Chen (2000). All samples remained in darkness to avoid any other contribution to  $\beta$ -carotene degradation. The  $\beta$ -carotene concentration (C) was determined in triplicate at selected times for 45 days. The initial  $\beta$ -carotene content ( $C_0$ ) was measured immediately after freeze-drying, and the results are expressed as the percent of remaining  $\beta$ -carotene ( $C/C_0$ , %).

A first-order kinetic model was used to study the degradation of  $\beta$ -carotene (Dhuique-Mayer et al., 2007; Spada et al., 2012), where the degradation rate is proportional to the

**Fig. 1** Amaranth milling diagram showing the milling conditions for native starch and starch enriched fraction



concentration at constant temperature (Eq. 2) which defines the reaction rate constant ( $k$ ). Arrhenius model was used to study the dependence of reaction rate constant ( $k$ ) with temperature  $T$  (Eq. 3) (Dhuique-Mayer et al., 2007).

$$C = C_0 \exp^{-kt} \quad (2)$$

$$k = k_{\infty} \exp^{-E_a/RT} \quad (3)$$

where  $k_{\infty}$  is the pre-exponential factor ( $s^{-1}$ ),  $E_a$  activation energy ( $J \text{ mol}^{-1}$ ), and  $R$  gas constant ( $J \text{ mol}^{-1} \text{ K}^{-1}$ ).

### Computer Vision System

Starchy matrix color changes were determined by image analysis, using the methodology developed by Agudelo-Laverde et al. (2013). The computer vision system (CVS) consisted of three elements: a lighting system, a digital camera and a

personal computer. The lighting system included a D65 lamp (this illuminant corresponds to solar irradiation with a color temperature of 6500 K (Agudelo-Laverde et al., 2013) inside a gray chamber (N7 in the Munsell color space). The time of warm up of the lamps was of 15 min before taking pictures. The angle between the camera axis and the sample plane was  $90^\circ$ , and the angle between the light source and the sample plane was  $45^\circ$ , in order to capture the diffuse reflection responsible for color, which is produced at this angle (Yam & Papadakis, 2004). A high-resolution (10.1 M-pixel) digital camera model EOS 40D (Canon Inc., Japan) was used, with an EF-S 60 mm f2.8 macro lens (Canon Inc.).

At selected times, the stored samples were transferred from the fridge ( $5^\circ \text{C}$ ) or the forced air oven ( $25$  and  $45^\circ \text{C}$ ) to the gray box for image acquisition. The digital camera was operated in manual mode, with the lens aperture at  $f6.3$  and speed  $1/8$  s (no zoom, no flash) to achieve high uniformity and

repeatability. The calibration of the camera and the parameters used for image capture are described in Briones & Aguilera (2005). Images have a resolution of  $3888 \times 2592$  pixels and were stored in JPEG format using Canon's Remote Capture program (EOS Utility, Canon Inc., USA). The images were taken using white background. CVS permitted acquiring information for the whole piece directly inside the glass vials. Color images were obtained in Lab values using Adobe Photoshop CS4 software (Adobe Systems Inc., San Jose, CA, USA) and then were converted to the standard CIELAB space using mathematical formulas described by Papadakis et al. (2000). The images of the matrices were segmented in two different parts, according to their  $a^*$  values: the red regions, attributed to surface  $\beta$ -carotene (with  $a^*$  values from 25 to 5), and the pinky regions, attributed to encapsulated  $\beta$ -carotene (with  $a^*$  values from 0 to 5).

### Statistical Analysis

Significance of  $\beta$ -carotene retention and stability was evaluated by one-way ANOVA (significance level  $\alpha = 0.05\%$ ) with Tukey's post-test using Prism 5 (GraphPad Software Inc., San Diego, CA, USA). In some cases,  $P$  value was calculated by a  $t$  test in order to further analyze the differences between samples.

## Results and Discussion

### Encapsulation Efficiency of Amaranth Matrices for $\beta$ -Carotene Encapsulation

The influence of matrix as well as the effect of ball milling treatment was evaluated on matrix encapsulation capability. Obtaining a stabilized emulsion is a previous step before freeze-drying. Figure 2 shows the amount of  $\beta$ -carotene emulsified by different matrices. It can be appreciated the better performance of SEF-based matrices to incorporate  $\beta$ -carotene in aqueous dispersion in comparison with NS fraction-based ones. The addition of Ge to SEF did not produce any further improvement in  $\beta$ -carotene incorporation, revealing the good properties of amaranth protein as emulsifiers. In contrast, the addition of Ge to the native starch milled fraction (NS-Ge/BM vs. NS/BM) improved  $\beta$ -carotene emulsification, but this effect was irrelevant in comparison to that of SEF/BM fraction. The ability of amaranth proteins, in particular globulin fractions, to emulsify water insoluble compounds have been reported by other authors (Avanza et al., 2005; Bejarano-Lujan et al., 2010; Condes et al., 2008), and they can be considered as a main factor of the encapsulation process.

The non-milled starch sample without gelatin (NS) presented unusual high emulsifying values, considering the low proportion of both amylose and short amylopectin chains. This

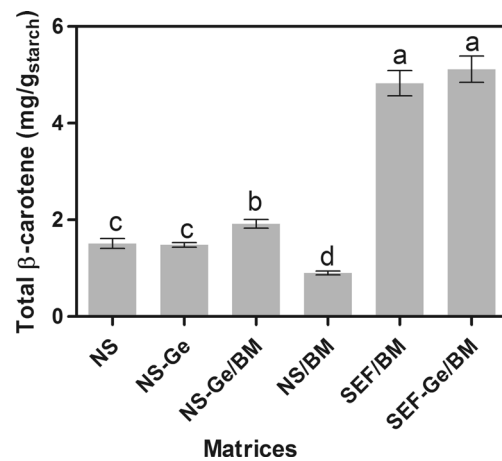


**Fig. 2** Amount of  $\beta$ -carotene emulsified in dispersions of different composition (starch fraction, processing—ball milling—and protein content/type). Standard deviation values are included. Different letters on the bars (a–d) indicate significant differences between mean values with  $P < 0.05$ . NS native starch, Ge gelatin, BM ball milling, SEF starch-enriched fraction

was attributed to the great heterogeneity of the sample after the dispersion, which could be seen by direct observation of red spots, making it inadequate for industrial applications.

Figure 3a shows the amounts of surface and encapsulated  $\beta$ -carotene found in the different studied systems. The effect of ball milling on  $\beta$ -carotene encapsulation can be observed by comparing NS and NS/BM samples: the sample NS/BM encapsulated 60% more than NS sample. The intense milling breaks the long chains of amylopectin into smaller size chains (Morrison et al., 1993), which could lead to a higher formation of  $\beta$ -carotene-starch inclusion complexes, and hence, more  $\beta$ -carotene was encapsulated. These authors demonstrated that those chains are even smaller than the amylose chains, which could provide the necessary movements so that the inclusion is more efficiently performed. Lokuwan (2007) encapsulated

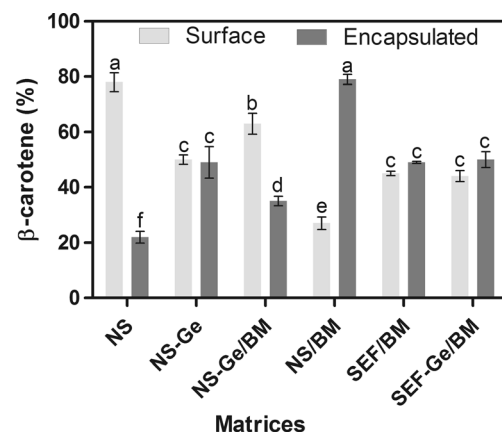


**Fig. 3** Surface and encapsulated  $\beta$ -carotene in gelatinized starch matrices of different compositions (starch fraction, processing—ball milling—and protein content/type). Standard deviations values are included. Different letters on the columns (a–f) indicate significant differences between mean values with  $P < 0.05$ . NS native starch, Ge gelatin, BM ball milling, SEF starch-enriched fraction

$\beta$ -carotene by spray drying on native and modified (hydrolyzed) starch tapioca matrices and obtained encapsulation degrees similar to those of this work, showing that the modified starch had better performance than the native starch. Besides the size reduction of amylopectin chains, an increase on the surface area of the powder (Roa et al., 2014) could also play part during encapsulation, thereby improving contact between starchy matrix and  $\beta$ -carotene. Matrices based on the SEF were able to encapsulate ~50% of  $\beta$ -carotene present in the emulsion, while the addition of gelatin to this fraction had no significant effect on the encapsulation (or during emulsification, as previously stated).

The stability index III/II% was obtained by analysis of the fine structure of the UV-Vis spectrum and reveals the structural state of carotenoids, indicating possible isomerizations or structural changes (Britton, 1995). The maximum absorption peaks remained at 478, 452, and 425 nm (Fig. S1 in Supplementary File), which are characteristic of the  $\beta$ -carotene (also called  $\beta,\beta$ -carotene) (Britton, 1995). Index values III/II% showed no significant variations in any of the employed matrices (values close to  $37.5 \pm 0.5\%$ ; Fig. S2 in Supplementary File), which means that the structure of both the encapsulated and surface  $\beta$ -carotene remained stable during processing.

Table 1 shows the encapsulation performance for each prepared matrix, defined as encapsulated to surface mass ratio of  $\beta$ -carotene. Table 1 demonstrates that milled matrices based on SEF and NS achieved yields higher than 1, improving encapsulation performance. However, the amount of encapsulated  $\beta$ -carotene must also be considered. NS/BM matrix contained one fifth of the  $\beta$ -carotene of the SEF matrices despite of its higher encapsulation performance.

It must be noted that a significant decrease of encapsulation performance (or increasing of surface  $\beta$ -carotene) was observed by addition of gelatin to NS/BM matrix (Fig. 3a). It seems that gelatin behaves as  $\beta$ -carotene stabilizer competing with milled starch for  $\beta$ -carotene encapsulation, resulting in an

increase of surface  $\beta$ -carotene, since these labile complexes are easily broken by agitation during  $\beta$ -carotene extraction.

The amount of encapsulated  $\beta$ -carotene in the SEF and SEF/BM matrices was higher than the ones found by Tari et al. (2003) when they encapsulated vanillin in amaranth starch using carboxymethyl cellulose and carrageenan as emulsifying agents, but it was slightly lower when they used guar gum. However, it is necessary to clarify that the difference between these results is also due to the different methods of encapsulation used.

Considering the results regarding the total amount of  $\beta$ -carotene incorporated during emulsification (Fig. 2), the encapsulation performance and the amount of encapsulated  $\beta$ -carotene per gram of starch (Fig. 3 and Table 1) and the structure index (Fig. S2) the encapsulation matrix selected for studying the effects of the storage temperature (5, 25, and 45 °C, during 45 days) on the retention of  $\beta$ -carotene as well as on color changes was SEF/BM.

### Thermal Stability of $\beta$ -Carotene Encapsulated on SEF-Based Amaranth Matrices

Carotenoids are prone to structural changes because they are highly unsaturated structures that may suffer the isomerization of their links going from *trans* to *cis* (for example, for  $\beta$ -carotene). When this happens, the carotenes lose their color and the pro-vitamin A activity (Fennema, 1996). The external factors that promote the isomerization are heat, light, and acids, among others (Kimura and Rodríguez-Amaya, 2001). The main degradation mechanism of the carotenoids in the presence of air or oxygen is the oxidation due to the high number of conjugated double links (Fennema, 1996). However, the degradation inside the encapsulation systems can occur depending on the type of material used as protector agent. The main degradation products are mono- and di-epoxides, carbonyls, and alcohols (Kimura & Rodríguez-Amaya, 2001).

**Table 1** Performance of different matrices on  $\beta$ -carotene encapsulation

| Matrices  | Surface $\beta$ -carotene (mg/g <sub>starch</sub> ) | Encapsulated $\beta$ -carotene (mg/g <sub>starch</sub> ) | Encapsulation performance <sup>a</sup> |
|-----------|-----------------------------------------------------|----------------------------------------------------------|----------------------------------------|
| NS        | 1.18 $\pm$ 0.09b                                    | 0.33 $\pm$ 0.01d                                         | 0.3 $\pm$ 0.1f                         |
| NS-Ge     | 0.84 $\pm$ 0.03c                                    | 0.64 $\pm$ 0.02b                                         | 0.76 $\pm$ 0.08d                       |
| NS/BM     | 0.37 $\pm$ 0.03d                                    | 0.53 $\pm$ 0.01c                                         | 1.4 $\pm$ 0.2a                         |
| NS-Ge/BM  | 1.23 $\pm$ 0.05b                                    | 0.69 $\pm$ 0.04b                                         | 0.6 $\pm$ 0.1de                        |
| SEF/BM    | 2.4 $\pm$ 0.2a                                      | 2.46 $\pm$ 0.08a                                         | 1.04 $\pm$ 0.09bc                      |
| SEF-Ge/BM | 2.4 $\pm$ 0.1a                                      | 2.7 $\pm$ 0.2a                                           | 1.1 $\pm$ 0.1ab                        |

For each column, different letters (a–f) indicate significant differences ( $P < 0.05$ ) between mean values

NS native starch, Ge gelatin, BM ball milling, SEF starch-enriched fraction

<sup>a</sup> Encapsulation performance: Mass ratio between encapsulated and surface  $\beta$ -carotene



Figure 4a, b describes the kinetics of the surface and encapsulated  $\beta$ -carotene in the milled starchy fraction (SEF/BM) stored at three temperatures (5, 25, and 45 °C) for 45 days.  $\beta$ -Carotene degradation was temperature-dependent, and higher degradation occurred at higher temperatures. A better protection was observed for the encapsulated  $\beta$ -carotene in comparison with that of the surface, especially at 45 and 25 °C. At 5 °C, there were no differences between encapsulated and surface  $\beta$ -carotene, showing more than 75% of retention after 45 days. The samples kept at 5 °C only after 17 days showed significant differences with respect to day 0, even though the retention values were still high ( $>93 \pm 4\%$ ). At 25 °C, surface  $\beta$ -carotene was totally degraded at day 24, while the encapsulated one retained  $33 \pm 4\%$  of the initial content, reaching  $14 \pm 4\%$  at the end of the study. Moreover, the increase of temperature to 45 °C quickly affected the degradation of surface and encapsulated  $\beta$ -carotene. Figure 4a shows that the surface  $\beta$ -carotene was already degraded on day 7, while the encapsulated  $\beta$ -carotene was  $29 \pm 3\%$  of the initial value (Fig. 4b), reflecting the protective capability of the SEF matrix even at high temperatures. At the end of the study, it was determined that only  $3.1 \pm 0.4\%$  of  $\beta$ -carotene encapsulated was still present on the samples.

The degradation of the  $\beta$ -carotene due to temperature was also studied by Desobry et al. (1997) in maltodextrin (DE = 25) matrices concluding that 80% of the  $\beta$ -carotene was degraded in 7 days at 45 °C, whereas samples stored at 25 °C retained 30% of  $\beta$ -carotene after the second week. Spada et al. (2012) studied the stability of the

microencapsulated  $\beta$ -carotene in *pinhao* (pine) starch (*Araucaria angustifolia*) by freeze-drying. These authors obtained high percentages of surface  $\beta$ -carotene (43%) when it was encapsulated with native starch, while it was of 12% employing hydrolyzed starch (up to an equivalent of DE = 12). Furthermore, they observed that the degradation of the  $\beta$ -carotene increased due to the temperature rise as well as by exposure to light. This degradation was an inverse function of the DE (higher degradation at lower DE), implying that a greater proportion of long-chain saccharides contributes in forming an inflexible barrier that is permeable to oxygen, increasing oxidation and degradation of the encapsulated compound (Wagner & Warthesen, 1995).

Furthermore, the influence of temperature on  $\beta$ -carotene structure was analyzed through the III/II% index. Figure 4c describes how the temperature notably affected the structure of the surface  $\beta$ -carotene compared to the encapsulated  $\beta$ -carotene (Fig. 4d), especially at storage temperatures above 25 °C, demonstrating the importance of encapsulation as a conservation and storage technique of labile molecules. Although it is not possible to say which isomerization occurs (there are potentially 272 possible isomers for  $\beta$ -carotene; Fennema, 1996) caused by temperature, changes are observed in the fine structure of the  $\beta$ -carotene spectrum (data not shown), especially affecting the length of the peak of the maximum wavelength.

The degradation of  $\beta$ -carotene (Fig. 4a, b) followed first-order kinetics (Lavelli et al., 2007; Spada et al., 2012; Sutter et al., 2007), and the ( $k_e$  and  $k_s$ ) constants values are shown in

**Fig. 4** Percent of remaining surface and encapsulated  $\beta$ -carotene (a, b) and stability index III/II% (c, d) of starch-enriched fraction (SEF) samples subjected to different storage temperatures. The III/II% index is the ratio between the height of the longest wavelength absorption peak (478 nm, designated as III) and the middle absorption peak (452 nm, designated as II), taking as the baseline the minimum between the two peaks. Experimental data (a, b) was fitted by a first order kinetic equation. Standard deviations values are included

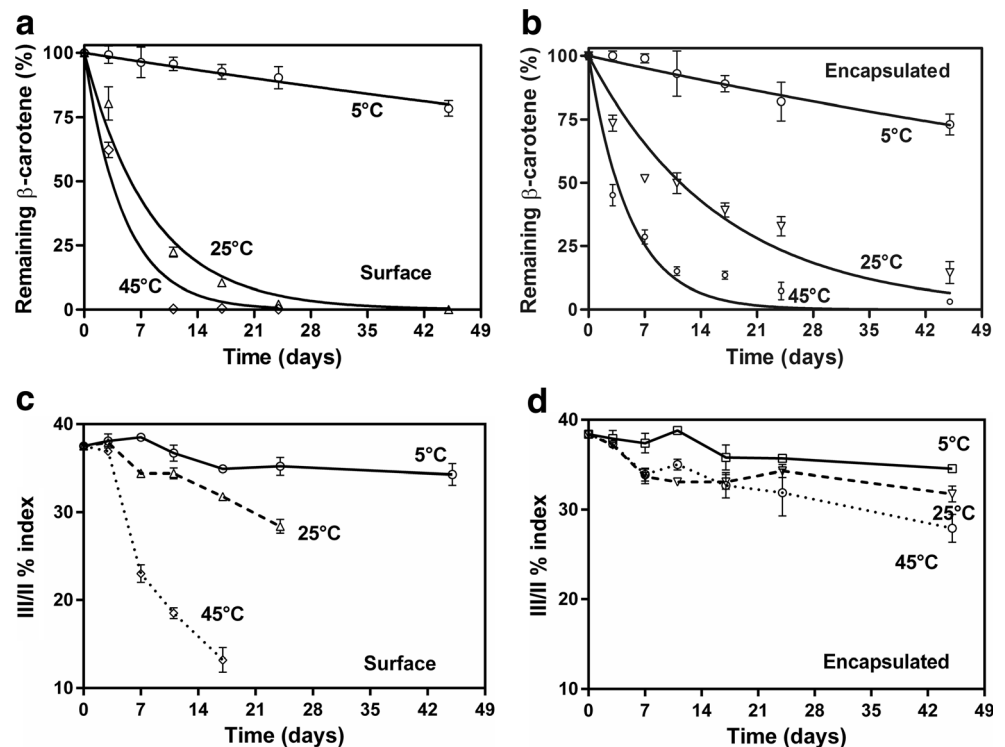


**Table 2** Degradation first order kinetics constants of surface ( $k_s$ ) and encapsulated ( $k_e$ )  $\beta$ -carotene at different temperatures

| Temperature (°C) | $k_s$ (days <sup>-1</sup> ) | $k_e$ (days <sup>-1</sup> ) |
|------------------|-----------------------------|-----------------------------|
| 5                | -0.0053 ± 0.0003e           | -0.0075 ± 0.0006f           |
| 25               | -0.16 ± 0.01b               | -0.039 ± 0.003d             |
| 45               | -0.6 ± 0.1a                 | -0.07 ± 0.01c               |

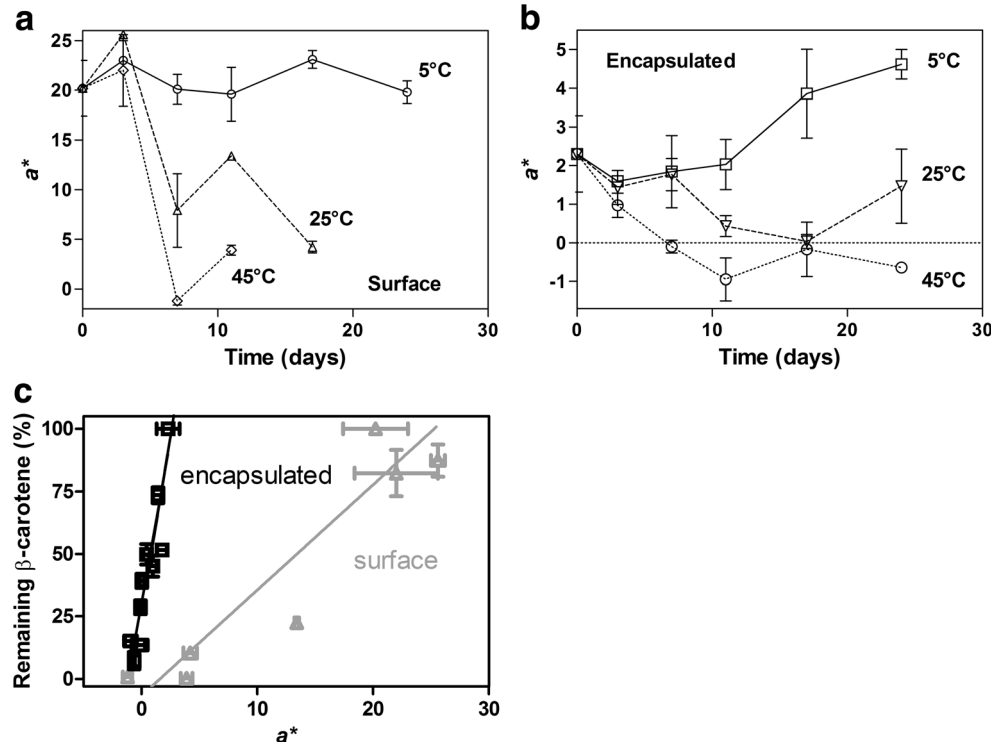
Different letters (a–f) indicate significant differences ( $P < 0.05$ ) between the mean values

Table 2. The values of the kinetic degradation constants of the surface  $\beta$ -carotene ( $k_s$ ) were higher than the degradation constant of the encapsulated ( $k_e$ ). The obtained constants were heavily influenced by the storage temperature, reflecting the lower temperature dependence for the conservation of the encapsulated  $\beta$ -carotene. It is interesting to highlight that the  $k_e$  at 45 °C (-0.07 ± 0.01) is even lower than the  $k_s$  (-0.16 ± 0.01) at 25 °C, clearly demonstrating a protective effect of the matrix on the encapsulated  $\beta$ -carotene. Arrhenius model was satisfactorily applied ( $r^2 > 0.95$ ) to fit the temperature effect on  $\beta$ -carotene degradation (Cisse et al., 2009; Hidalgo & Brandolini, 2008). The values of activation energy ( $E_a$ ) were 86 and 48 ± 6 kJ/mol for the surface and encapsulated  $\beta$ -carotene, respectively. These values are relatively similar to those reported in the bibliography describing the surface or non-encapsulated  $\beta$ -carotene (Bechoff et al., 2011; Dhuique-Mayer et al., 2007). The greatest  $E_a$  obtained

for the surface  $\beta$ -carotene vs. the encapsulated implies that the degradation of encapsulated  $\beta$ -carotene is less temperature dependent and, thus, more stable to temperature changes than surface  $\beta$ -carotene.

Finally, the temperature effect on CIELAB ( $L^*$ ,  $a^*$ ,  $b^*$ ) color coordinates obtained from the images of freeze-dried matrices was analyzed. In order to evaluate the contribution of surface and encapsulated  $\beta$ -carotene degradation to the color changes during storage at different temperatures, the images were segmented obtaining an average  $a^*$  value representative of the reddish zones (corresponding to surface  $\beta$ -carotene) and another value corresponding to the less saturated pinky zones of the matrices (corresponding to encapsulated  $\beta$ -carotene). Results showed significant difference between the surface and encapsulated  $\beta$ -carotene, especially at 25 and 45 °C. Figure 5a describes how the temperature markedly affected  $a^*$  values of the surface  $\beta$ -carotene compared to the encapsulated  $\beta$ -carotene (Fig. 5b). Encapsulated  $\beta$ -carotene depicted much lower decrease of  $a^*$  values than the surface one, revealing the protective effect of the matrix, in accordance with the results discussed in the previous section. After 7 days of storage,  $a^*$  value decreased for surface  $\beta$ -carotene (Fig. 5b) because the reddish chromaticity provided by  $\beta$ -carotene decreased due to its degradation. The coordinate  $L^*$  increased (Fig. S3 of Supplementary File) parallel to visually perceived lightening, while the chromatic coordinate  $b^*$  was also significantly different in surface and encapsulated  $\beta$ -carotene (Fig. S4 of Supplementary File), following a

**Fig. 5** Chromatic coordinate  $a^*$  of surface (a) and encapsulated (b)  $\beta$ -carotene on freeze-dried starchy matrices during storage at 5, 25, and 45 °C. The images were segmented in order to obtain  $a^*$  values of the reddish zones (corresponding to surface  $\beta$ -carotene) and of the less saturated zones of the matrices (corresponding to encapsulated  $\beta$ -carotene). c Correlation of  $a^*$  values with remaining  $\beta$ -carotene (from Fig. 4a, b) from samples stored at 25 and 45 °C



similar trend to  $a^*$ .  $L^*$  and  $a^*$  coordinates have been previously proposed as the most sensitive parameters to depict encapsulated  $\beta$ -carotene degradation in maltodextrin and starch matrices (Desobry et al., 1997; Spada et al., 2012).

While at 5 °C the three chromatic coordinates slightly changed (only 10% of  $\beta$ -carotene was lost at this temperature), the data obtained from color measurement ( $a^*$  and  $L^*$ ) for samples stored at 25 and 45 °C positively correlated with the remaining  $\beta$ -carotene determined from the hexane extract as shown in Fig. 5c and Fig. S5, respectively. The  $R^2$  values were higher than 0.84 in all cases, revealing the potentiality of color measurement as an adequate index of prediction of  $\beta$ -carotene retention stored at 25 and 45 °C on starchy matrices.

## Conclusions

Ball milling is a simple process, presenting minimal environmental problems and it is easy to operate. In addition, adopting milling energy as independent variable, instead of milling-speed and milling-time combinations, both dependent on milling protocol and equipment, could facilitate scaling up.

Through a high energy milling technique, such as planetary ball milling, it was possible to produce an amaranth fraction (88% starch, 5% proteins), potentially of great technological value, which can be used as carotenoids encapsulation matrix and other related compounds, for food and non-food applications. In addition to the already recognized and valuable properties of this fraction (low particle size and crystallinity degree, and high water absorption and solubility indexes), the amaranth proteins play a key role in the emulsification of  $\beta$ -carotene, providing better emulsification efficiency than gelatin.

$\beta$ -Carotene encapsulated in SEF matrices showed an improved thermal stability than the one on the surface, revealing the capability of this fraction as an encapsulation material at different temperatures.

Colorimetric analysis proved to be a useful non-destructive tool for evaluating  $\beta$ -carotene degradation at 25 and 45 °C, particularly  $a^*$  and  $L^*$  coordinates. However, it has to be taken into account that the global change of the color is measured, not only the one attributed to  $\beta$ -carotene (since oxidation products are often colored). The segmentation procedure for separating surface and encapsulated  $\beta$ -carotene in the images through processing software is quite laborious but can help to improve the evaluation of the remaining  $\beta$ -carotene in the different spatial portions of the samples, avoiding the use of organic solvents and complicated extraction procedures, if the corresponding validations are performed.

This study contributes expanding the possible uses of amaranth, a pseudocereal produced in Andean region in South America, with the concomitant economical opportunities.

**Acknowledgements** The authors acknowledge the financial support from UBACYT (Project UBACYT 20020100100397 and 20020130100442BA) and ANPCYT (PICT 2013-0434 and PICT 2013-1331). PRS and MPB are members of CONICET, Argentina.

## References

- Agudelo-Laverde, L., Schebor, C., & Buera, M. P. (2013). Water content effect on the chromatic attributes of dehydrated strawberries during storage, as evaluated by image analysis. *LWT-Food Science and Technology*, 52, 157–162.
- Association of Official Analytical Chemists (2000). AOAC 925.09. Solids (total) and moisture in flour. In *Official methods of analysis* (17th ed.). Gaithersburg, MD: Association of Official Analytical Chemists.
- Avanza, M. V., Puppo, M. C., & Añón, M. C. (2005). Rheological characterization of amaranth protein gels. *Food Hydrocolloids*, 19(5), 889–898.
- Bechoff, A., Tomlins, K., Dhuique-Mayer, C., Dove, R., & Westby, A. (2011). On-farm evaluation of the impact of drying and storage on the carotenoid content of orange-fleshed sweet potato (*Ipomea batata* Lam.). *International Journal of Food Science & Technology*, 46, 52–60.
- Bejarano-Luján, D. L., Lopes da Cunha, R., & Netto, F. M. (2010). Structural and rheological properties of amaranth protein concentrate gels obtained by different processes. *Food Hydrocolloids*, 24, 602–610.
- Breene, W. M. (1991). Food uses of grain Amaranth. *Cereal Foods World*, 36, 426–430.
- Briones, V., & Aguilera, J. M. (2005). Image analysis of changes in surface color of chocolate. *Food Research International*, 38(1), 87–94.
- Britton, G. (1995). UV/visible spectroscopy. In G. Britton, S. Liaaen-Jensen, & H. Pfander (Eds.), *Carotenoids* (pp. 13–62). Basel: Birkhäuser.
- Chattopadhyaya, S., Singhal, R. S., & Kulkarni, P. R. (1998). Oxidised starch as gum Arabic substitute for encapsulation of flavours. *Carbohydrate Polymers*, 37, 143–144.
- Chen, J., Lii, Y., & Lu, S. (2003). Physicochemical and morphological analyses on damaged rice starches. *Journal of Food and Drug Analysis*, 11, 283–289.
- Choi, H., Kim, W., & Shin, M. (2004). Properties of Korean amaranth starch compared to waxy millet and waxy sorghum starches. *Starch*, 56, 469–477.
- Cisse, M., Vaillant, F., Acosta, O., Dhuique-Mayer, C., & Domier, M. (2009). Thermal degradation kinetics of anthocyanins from blood orange, blackberry, and roselle using the Arrhenius, Eyring, and Ball models. *Journal of agricultural and food chemistry*, 14, 6285–6291.
- Condes, M., Scilingo, A., & Añón, M. (2008). Characterization of amaranth proteins modified by trypsin proteolysis. Structural and functional changes. *LWT-Food Science and Technology*, 42, 963–970.
- Desobry, S. A., Netto, F. M., & Labuza, T. P. (1997). Comparison of spray-drying, drum drying and freeze-drying for  $\beta$ -carotene encapsulation and preservation. *Journal Food Science*, 62, 1158–1162.
- Devi, F., Fibrianto, K., Torley, J., & Bhandari, B. (2009). Physical properties of cryomilled rice starch. *Journal of Cereal Science*, 49, 278–284.
- Dhuique-Mayer, C., Tbatou, M., Carail, M., Caris-Veyrat, C., Domier, M., & Amiot, M. (2007). Thermal degradation of antioxidant micronutrients in citrus juice: kinetics and newly formed compounds. *Journal of Agricultural and Food Chemistry*, 55, 4209–4216.

- Fennema, O. (1996). In O. Fennema (Ed.), *Food chemistry* (third ed.). New York: Marcel Dekker, Inc..
- Hidalgo, A., & Brandolini, A. (2008). Kinetics of carotenoids degradation during the storage of einkorn (*Triticum monococcum* L. ssp. *monococcum*) and bread wheat (*Triticum aestivum* L. ssp. *aestivum*) flours. *Journal of Agricultural and Food Chemistry*, *56*, 11300–11305.
- Huang, Z., Lu, J., Li, X., & Tong, Z. (2007). Effect of mechanical activation on physico-chemical properties and structure of cassava starch. *Carbohydrate Polymer*, *68*, 128–135.
- Jane, J., Shen, L., Wang, L., & Maningat, C. C. (1992). Preparation and properties of small-particle corn starch. *Cereal Chemistry*, *69*, 280–283.
- Karathanos, V. T., Mourtzinou, I., Yannakopoulou, K., & Andrikopoulos, N. K. (2007). Study of the solubility, antioxidant activity and structure of inclusion complex of vanillin with  $\beta$ -cyclodextrin. *Food Chemistry*, *101*, 652–658.
- Kimura, M., & Rodriguez-Amaya, D. B. (2001). A scheme for obtaining standards and HPLC quantification of leafy vegetable carotenoids. *Food Chemistry*, *78*, 389–398.
- Kong, X., Kasapis, S., Bao, J., & Corke, H. (2008). Effect of gamma irradiation on the thermal and rheological properties of grain amaranth starch. *Radiation Physics and Chemistry*, *78*, 954–960.
- Krishnan, S., Bhosale, R., & Singhal, R. (2005). Microencapsulation of cardamom oleoresin: Evaluation of blends of gum arabic, maltodextrin and a modified starch as wall materials. *Carbohydrate Polymers*, *61*, 95–102.
- Lavelli, V., Zanoni, B., & Zaniboni, A. (2007). Effect of water activity on carotenoid degradation in dehydrated carrots. *Food Chemistry*, *104*, 1705–1711.
- Loksuwan, J. (2007). Characteristics of microencapsulated  $\beta$ -carotene formed by spray drying with modified tapioca starch, native tapioca starch and maltodextrin. *Food Hydrocolloids*, *21*, 928–935.
- Madene, A., Jacquot, M., Scher, J., & Desobry, S. (2006). Flavour encapsulation and controlled release. *International Journal of Food Science and Technology*, *41*, 1–21.
- Marcone, M. F. (2001). Starch properties of *Amaranthus pumilus* (seabeach amaranth): a threatened plant species with potential benefits for the breeding/amelioration of present amaranth cultivars. *Food Chemistry*, *71*, 61–66.
- Matioli, G., & Rodriguez-Amaya, D. (2002). Licopeno encapsulado em goma arábica e maltodextrina: estudo da estabilidade. *Brazilian Journal of Food Technology*, *5*, 197–203.
- Morrison, W. R., Tester, R. F., Snape, C. E., Law, R., & Gidley, M. J. (1993). Swelling and gelatinization of cereal starches. IV. Some effects of lipid-complexed amylose and free amylose in waxy and normal barley starches. *Cereal Chemistry*, *70*, 385–391.
- Morrison, W. R., & Tester, R. F. (1994). Properties of damaged starch granules. IV. Composition of ball-milled wheat starches and of fractions obtained on hydration. *Journal of Cereal Science*, *20*, 69–77.
- Murúa-Pagola, B., Beristain-Guevara, C. I., & Martínez-Bustos, F. (2009). Preparation of starch derivatives using reactive extrusion and evaluation of modified starches as shell materials for encapsulation of flavoring agents by spray drying. *Journal of Food Engineering*, *91*, 380–386.
- Papadakis, S. E., Abdul-Malek, S., Kamdem, R. E., & Yam, K. L. (2000). A versatile and inexpensive technique for measuring color of foods. *Food Technology*, *54*, 48–51.
- Puncha-amon, S., & Uttapap, D. (2013). Rice starch vs. rice flour: differences in their properties when modified by heat–moisture treatment. *Carbohydrate Polymer*, *91*, 85–91.
- Radosavljevic, M., Jane, J., & Johnson, J. (1998). Isolation of amaranth starch by diluted alkaline protease treatment. *Cereal Chemistry*, *75*, 212–216.
- Roa, D. F., Baeza, R. I., & Tolaba, M. P. (2015). Effect of ball milling energy on rheological and thermal properties of amaranth flour. *Journal of Food Science and Technology*, *52*, 8389–8394.
- Roa, D. F., Santagapita, P. R., Buera, M. P., & Tolaba, M. P. (2013). Amaranth milling strategies and fraction characterization by FT-IR. *Food and Bioprocess Technology*, *7*, 711–718.
- Roa, D. F., Santagapita, P. R., Buera, M. P., & Tolaba, M. P. (2014). Ball milling of Amaranth starch-enriched fraction. Changes on particle size, starch crystallinity, and functionality as a function of milling energy. *Food and Bioprocess Technology*, *7*, 2723–2731.
- Sanguanpong, V., Chotineerant, S., Piyachomkwan, K., Oates, C., Chinachoti, P., & Sriroth, K. (2003). Preparation and structural properties of small-particle cassava starch. *Journal of the Science of Food and Agriculture*, *83*, 760–768.
- Saunders, R., & Becker, R. (1984). Amaranthus: a potential food and feed resource. In Pomeranz (Ed.), *Advances in cereal science and technology* (pp. 357–396). St Paul, MN: American Association of Cereal Chemists.
- Silva, D., Couturier, M., Berrin, J., Buleon, A., & Rouau, X. (2012). Effects of grinding processes on enzymatic degradation of wheat straw. *Bioresource Technology*, *103*, 192–200.
- Spada, J., Marczak, L., Tessaro, I., & Noreña, C. (2012). Microencapsulation of  $\beta$ -carotene using native pinhao starch, modified pinhao starch and gelatin by freeze-drying. *International Journal of Food Science and Technology*, *47*, 186–194.
- Sutter, C., Buera, M., & Elizalde, B. (2007).  $\beta$ -Carotene encapsulation in a mannitol matrix as affected by divalent cations and phosphate anion. *International Journal of Pharmaceutics*, *332*, 45–54.
- Tamaki, S., Hisamatsu, M., Teranishi, K., Adachi, T., & Yamada, T. (1998). Structural change of maize starch granules by ball-mill treatment. *Starch/Stärke*, *50*, 342–348.
- Tang, Y. C., & Chen, B. H. (2000). Pigment change of freeze-dried carotenoid powder during storage. *Food Chemistry*, *69*, 11–17.
- Tari, A., Uday, S., Annapure, S., Singhal, S., & Pushpa, R. (2003). Starch-based spherical aggregates: screening of small granule sized starches for entrapment of a model flavouring compound, vanillin. *Carbohydrate Polymers*, *53*, 45–51.
- Wagner, L., & Warthesen, J. (1995). Stability of spray-dried encapsulated carrot carotenes. *Journal of Food Science*, *60*, 1048–1052.
- Yam, K. L., & Papadakis, S. E. (2004). A simple digital imaging method for measuring and analyzing color of food surfaces. *Journal of Food Engineering*, *61*, 137–142.
- Zhang, Z., Zhao, S., & Xiong, S. (2010). Morphology and physicochemical properties of mechanically activated rice starch. *Carbohydrate Polymer*, *79*, 341–348.